

Dynamical Mass Generation and Confinement in Maxwell-Chern-Simons Planar Quantum Electrodynamics

S Sánchez Madrigal¹, C P Hofmann² and A Raya¹,

¹Instituto de Física y Matemáticas, Universidad Michoacana de San Nicolás de Hidalgo, Edificio C-3, Ciudad Universitaria, Morelia, Michoacán 58040, México.

²Facultad de Ciencias, Universidad de Colima, Bernal Díaz del Castillo 340, Colima, Colima 28045, México.

E-mail: saul@ifm.umich.mx, christoph@uicol.mx, raya@ifm.umich.mx,

Abstract. We study the non-perturbative phenomena of Dynamical Mass Generation and Confinement by truncating at the non-perturbative level the Schwinger-Dyson equations in Maxwell-Chern-Simons planar quantum electrodynamics. We obtain numerical solutions for the fermion propagator in Landau gauge within the so-called rainbow approximation. A comparison with the ordinary theory without the Chern-Simons term is presented.

1. Motivation

Dynamical Mass Generation (DMG) and Confinement are two emergent phenomena of Quantum Chromodynamics (QCD) responsible for the nature of the hadronic spectrum. These can be studied by means of the corresponding Schwinger-Dyson Equations (SDE), as an alternative to the formulation of QCD on the lattice. The SDEs form an infinite tower of relations among the Green's functions of a given quantum field theory, whose nature is genuinely non-perturbative. We choose to study the SDE in a simplified model that shares with QCD the phenomena of Confinement and DMG, namely, quantum electrodynamics in the plane, or QED₃. Applications of QED₃ also extend to condensed matter systems, including high-T_c superconductivity, the quantum Hall effect and, very recently, graphene. Moreover, it is interesting to include the Chern-Simons (CS) term for the gauge field, which explicitly breaks parity and induces a topological mass for the photons.

Incorporating the CS term in studies of DMG in QED₃ have found that when the CS coefficient reaches a critical value, chiral symmetry is restored in a first order phase transition [1, 2]. In this work, we are interested in the effect of the CS term regarding confinement in quenched QED₃. In Sec. 2 we present our model with a reducible representation of (2+1)-dimensional quantum electrodynamics with a CS term. Solutions to the gap equation in the rainbow approximation are presented in Sec. 3. The question of confinement in QED₃ with a CS term is addressed in Sec.4. Finally, in Sec. 5, we present our conclusions.

2. Model

We study quantum electrodynamics in (2+1)-dimensions. For fermions, there exist two irreducible representations of the Euclidean Clifford algebra $\{\gamma_\mu, \gamma_\nu\} = 2\delta_{\mu\nu}$. In any of these representations, it is impossible to define chiral symmetry [3, 4, 5]. Furthermore, the fermion mass term, regardless its origin, is parity \mathcal{P} non invariant. One still can construct a parity-preserving Lagrangian considering two different species with a relative sign between their masses [6, 7]. As a result, two chiral transformations can be defined [7]. These two species are conveniently merged into a single four-component spinor, making use of a reducible representation of the Dirac matrices. As compared with its four-dimensional counterpart, only three Dirac matrices are required to describe the dynamics of planar fermions. Once we have selected a set of matrices to write down the Dirac equation, say $\{\gamma_0, \gamma_1, \gamma_2\}$, two anti-commuting gamma matrices, namely, γ_3 and γ_5 remain unused. Hence the corresponding massless Dirac Lagrangian is invariant under the chiral-like transformations $\psi \rightarrow e^{i\alpha\gamma_3}\psi$ and $\psi \rightarrow e^{i\beta\gamma_5}\psi$, that is, it is invariant under a global $U(2)$ symmetry with generators 1, γ_3 , γ_5 and $[\gamma_3, \gamma_5]$, corresponding to the interchange of fermion species. This symmetry is broken by an ordinary mass term $m_e\bar{\psi}\psi$. The order parameter of the symmetry breaking is the condensate $\langle\bar{\psi}\psi\rangle_e = \langle 0|\bar{\psi}\psi|0\rangle$. There exists a second mass term which is invariant under the "chiral" transformations, referred to as the Haldane mass term $m_o\bar{\psi}\tau\psi$ [8] with $\tau = [\gamma_3, \gamma_5]/2 = \text{diag}(I, -I)$, which is associated with the condensate $\langle\bar{\psi}\psi\rangle_o = \langle 0|\bar{\psi}\tau\psi|0\rangle$. The ordinary mass term is even under parity \mathcal{P} transformations, but the Haldane mass term is not. We use the subscripts e for even and o for odd in quantities of the model. The Haldane mass term radiatively induces a parity-odd contribution into the vacuum polarization, which can be traced back to an induced Chern-Simons interaction

$$\mathcal{L}_{CS} = -\frac{i\theta}{4}\varepsilon_{\mu\nu\rho}A_\mu F_{\nu\rho}. \quad (1)$$

Such a term is parity non invariant, and despite the fact that it is not manifestly gauge invariant, the corresponding action respects gauge symmetry. The parameter θ induces a topological mass for the photons. Thus, the model we consider is described by the Lagrangian

$$\mathcal{L} = \bar{\psi}(i\cancel{\partial} + e\cancel{A} + m_e + \tau m_o)\psi + \frac{1}{4}F_{\mu\nu}F_{\mu\nu} + \frac{1}{2\xi}(\partial_\mu A_\mu)^2 - \frac{i\theta}{4}\varepsilon_{\mu\nu\rho}A_\mu F_{\nu\rho}. \quad (2)$$

There are many condensed matter systems which can be described by this Lagrangian, for which the physical origin of the masses depends on the underlying system, including high- T_c superconductivity, the quantum Hall effect and, very recently, graphene.

Written in this form, neither m_e nor m_o correspond to poles of the fermion propagator. We introduce the chiral projectors $\chi_\pm = (1 \pm \tau)/2$ which have the properties $\chi_\pm^2 = \chi_\pm$, $\chi_+\chi_- = 0$, $\chi_+ + \chi_- = 1$. These allow us to define the right-handed ψ_+ and left-handed ψ_- fermion fields as $\psi_\pm = \chi_\pm\psi$. The χ_\pm project the upper and lower two component spinors (fermion species) out of the four-component ψ , such that the fermion sector of the Lagrangian (2) can be cast in the form

$$\mathcal{L}_F = \bar{\psi}_+(i\cancel{\partial} - m_+)\psi_+ + \bar{\psi}_-(i\cancel{\partial} - m_-)\psi_-, \quad (3)$$

with $m_\pm = m_e \pm m_o$. This Lagrangian describes two fermion species of physical masses m_+ and m_- , respectively. These masses break chiral symmetry and parity at the same time. Moreover, the effect of the parity-violating mass is seen to remove the mass degeneracy between the two species. In what follows, we will be interested in the analytical properties of the dynamically generated fermion propagator associated with these physical masses. The analytical structure of the propagator can be studied from the corresponding Schwinger-Dyson equation, which corresponds to the expression

$$S_F(p)^{-1} = S_F^{(0)}(p)^{-1} + e^2 \int \frac{d^3k}{(2\pi)^3} \Gamma^\mu(k, p) S_F(k) \gamma^\nu \Delta_{\mu\nu}(k - p), \quad (4)$$

where $\Gamma^\mu(k, p)$ and $\Delta_{\mu\nu}(k - p)$ are, respectively, the full fermion-photon vertex and the full photon propagator, which obey themselves their own SDE, and $S_F(p)$ and $S_F^{(0)}(p)$ stand for the full and bare fermion propagator. In QED₃, the coupling e^2 has mass-dimension one. Moreover, since the theory is super-renormalizable, e^2 becomes the natural scale of massless QED₃, which is directly connected to the scales of confinement and dynamical chiral symmetry breaking. In this work, we write the relevant mass scales in units of $e^2 = 1$.

From the Lagrangian (2), we observe that inverse fermion propagator has the form

$$S_F^{-1}(p) = A_e(p)\not{p} + A_o(p)\tau\not{p} - B_e(p) - B_o(p)\tau. \quad (5)$$

The scalar functions $A_{e,o}(p)$ and $B_{e,o}(p)$ can be expressed in terms of the fermion wavefunction renormalizations $F_{e,o}(p)$ and the mass function $M_{e,o}(p)$ as $A_{e,o}(p) = 1/F_{e,o}(p)$ and $B_{e,o}(p) = M_{e,o}(p)/F_{e,o}(p)$ both in the even and odd sectors. The bare propagator corresponds to the values $A_e^{(0)}(p) = 1$, $A_o^{(0)}(p) = 0$, $B_e^{(0)}(p) = m_e$, $B_o^{(0)}(p) = m_o$. Rather than working with parity eigenstates, we find it convenient to work with the chiral Lagrangian (3). The chiral decomposition of the fermion propagator becomes

$$\begin{aligned} S_F(p) &= -\frac{A_+(p)\not{p} + B_+(p)}{A_+^2(p)p^2 + B_+^2(p)}\chi_+ - \frac{A_-(p)\not{p} + B_-(p)}{A_-^2(p)p^2 + B_-^2(p)}\chi_- \\ &\equiv -[\sigma_+^V(p)\not{p} + \sigma_+^S(p)]\chi_+ - [\sigma_-^V(p)\not{p} + \sigma_-^S(p)]\chi_-, \end{aligned} \quad (6)$$

where $K_\pm = K_e \pm K_o$ for all relevant even and odd quantities of the model. The inverse transformations are simply $K_e = (K_+ + K_-)/2$ and $K_o = (K_+ - K_-)/2$. In this basis, the bare quantities are $A_\pm^{(0)}(p) = 1$ and $B_\pm^{(0)}(p) = m_\pm$. On the other hand, the photon propagator associated with the Lagrangian (2) in the Landau gauge, $\xi = 0$, takes the form

$$\Delta_{\mu\nu}^{(0)}(q) = \frac{1}{q^2 + \theta^2} \left(\delta_{\mu\nu} - \frac{q_\mu q_\nu}{q^2} \right) - \frac{\varepsilon_{\mu\nu\rho} q_\rho \theta}{q^2(q^2 + \theta^2)}. \quad (7)$$

3. Gap Equation

We consider the rainbow-ladder truncation scheme, in which one makes the replacements $\Gamma^\mu \rightarrow \gamma^\mu$ and $\Delta_{\mu\nu} \rightarrow \Delta_{\mu\nu}^{(0)}$. With the chiral decomposition of the fermion propagator, Eq. (6), both in the left- and right-handed sector, the SDE corresponds to a matrix equation which can be converted into a system of scalar equations for $A_\pm(p)$ and $B_\pm(p)$ after multiplying it by 1 and \not{p} and taking the trace. In the limit $m_\pm = 0$, this leads to the decoupled system of equations

$$\begin{aligned} A_\pm(p) &= 1 + \frac{\alpha}{\pi^2 p^2} \int d^3k \sigma_\pm^V(k) \frac{(k \cdot q)(p \cdot q)}{q^2(q^2 + \theta^2)} \mp \frac{\alpha\theta}{\pi^2 p^2} \int d^3k \sigma_\pm^S(k) \frac{(p \cdot q)}{q^2(q^2 + \theta^2)}, \\ B_\pm(p) &= \frac{\alpha}{\pi^2} \int d^3k \sigma_\pm^S(k) \frac{1}{(q^2 + \theta^2)} \mp \frac{\alpha\theta}{\pi^2} \int d^3k \sigma_\pm^V(k) \frac{(k \cdot q)}{q^2(q^2 + \theta^2)}, \end{aligned} \quad (8)$$

with $\alpha = 1/(4\pi)$ as usual. Because of the effects of the CS term, the $A_\pm(p)$ functions become not trivial. Thus, in covariant gauges these never decouple from the equations for $B_\pm(p)$ as long as $\theta \neq 0$. We numerically solve the above systems of equations in each sector varying θ .

In Fig. 1 we show the functions $A_\pm(p)$ for different values of θ . The small deviation from the tree-level value for small momentum in each case is due to the CS term. As θ increases, both functions exhibit a plateau for small p and smoothly tend to 1 in the ultraviolet. The deviation is more pronounced in $A_-(p)$. Figure 2 shows the result for $B_\pm(p)$. We observe that the height of the plateau of $B_+(p)$ at small momentum decreases from the parity-even result as θ gets bigger, but the height of the plateau of $B_-(p)$ exhibits the opposite behavior. The effect

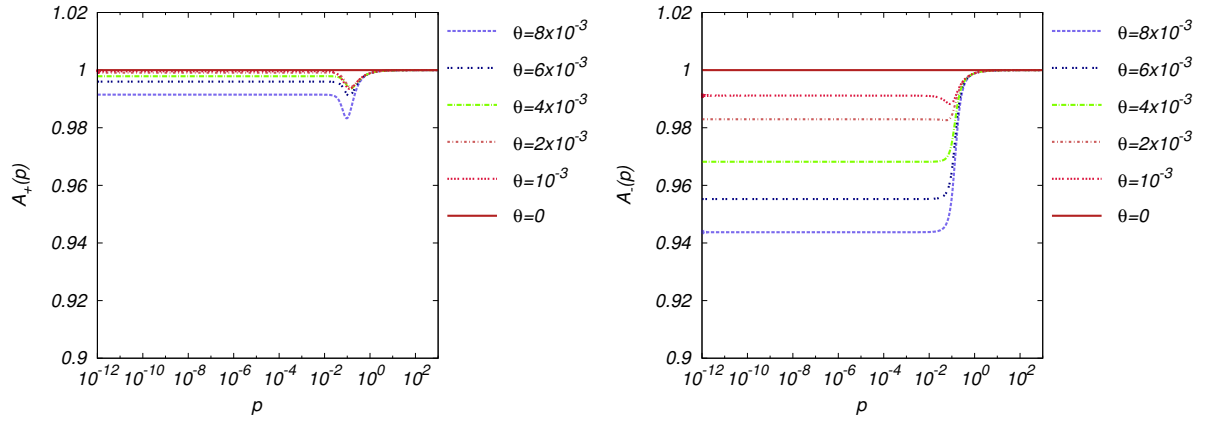


Figure 1. Functions $A_{\pm}(p)$ for various values of θ .

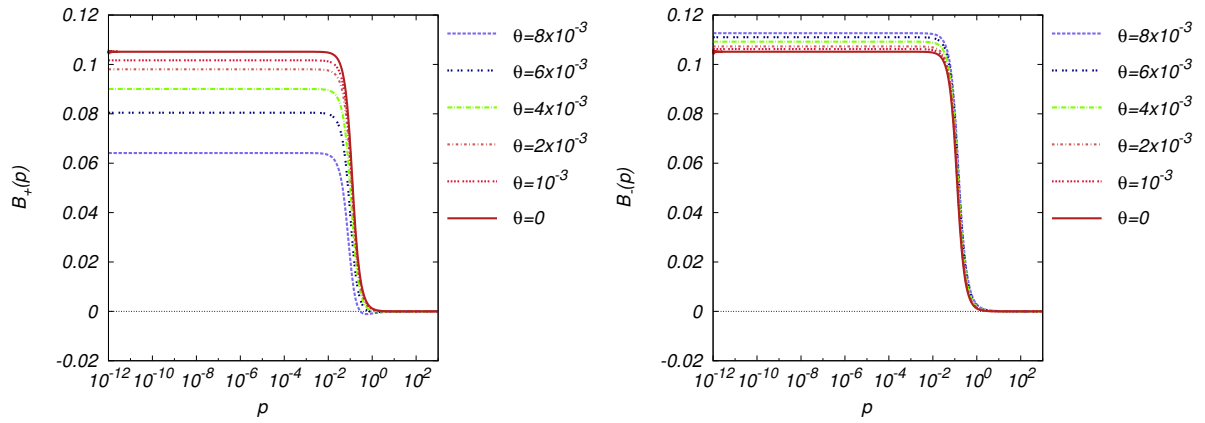


Figure 2. Functions $B_{\pm}(p)$ for various values of θ .

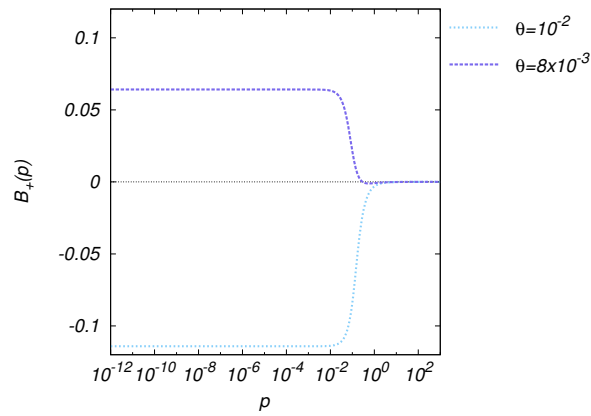


Figure 3. Critical behavior of $B_+(p)$ for $\theta \simeq 8 \times 10^{-3}$.

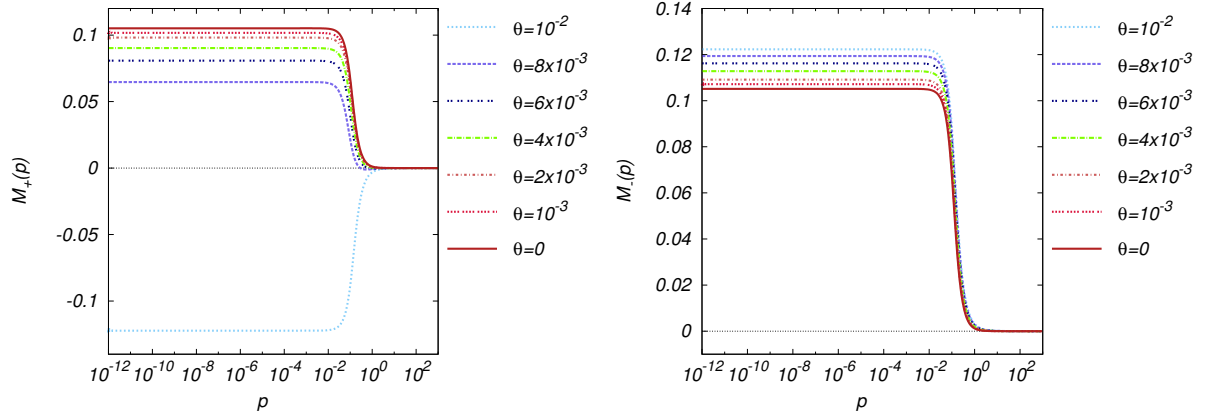


Figure 4. Mass functions $M_{\pm}(p)$ for various values of θ .

is more visible in $B_+(p)$. In fact, there is a critical value $\theta_c \simeq 8 \times 10^{-3}$ above which $B_+(p)$ strongly changes its behavior and the plateau becomes negative, as shown in Fig. 3.

This sudden drop has strong implications regarding chiral symmetry restoration in the model [1, 2]. In order to illustrate this, in Fig. 4, we show the mass functions $M_{\pm}(p) = B_{\pm}(p)/A_{\pm}(p)$ for different values of θ . At θ_c , the plateau of $M_+(p)$ also drops to negative values, whereas for $M_-(p)$, it continues to increase with θ . To ensure that these results are physically sensitive, we study the asymptotic behavior of $M_{\pm}(p)$. In the infrared, the height of the plateau can be considered as an order parameter for dynamical chiral symmetry breaking. In this connection, in Fig. 5 we draw the dependence of $\mu_{\pm} = M_{\pm}(0)$ as a function of θ below and above criticality. This parameter can be regarded as the dynamical mass of the corresponding fermion species. We observe that the role of the CS coefficient is to remove the mass degeneracy between fermion species as long as $\theta < \theta_c$. There is a light and a heavy species. At θ_c , however, there is a drastic change in this behavior, the light species develops a negative mass, which in absolute value is the same as its heavy cousin, as can be appreciated in the dotted curve in the same graph. This implies that above this θ_c , the would-be parity preserving mass $\mu_e = (\mu_+ + \mu_-)/2$ vanishes, and hence chiral symmetry is restored [1, 2]. Nevertheless, we want to emphasize that in this model, μ_e does not correspond to a pole in a propagator and hence to a physical mass. Physical masses μ_{\pm} are generated for arbitrarily large values of θ .

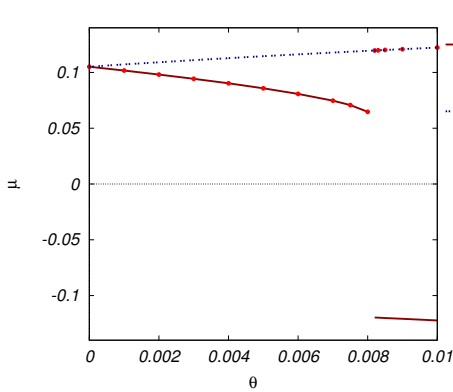


Figure 5. μ_{\pm} as a function of θ .

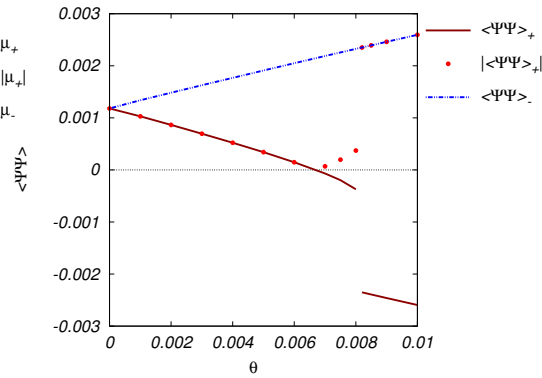


Figure 6. Chiral condensates as a function of θ .

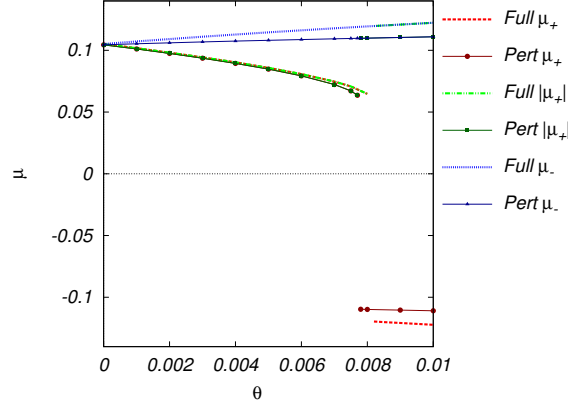


Figure 7. Comparison of the dynamically generated fermion masses for the full system (8) and the perturbatively reduced system (10).

The discontinuous behavior of the dynamically generated masses suggest a first order phase transition for the dynamical breaking of chiral symmetry. Whether there is chiral symmetry restoration can better be seen from the behavior of the condensates, which are the true order parameters. These can be extracted from the solution to the SDEs as

$$\langle \bar{\psi}\psi \rangle_{\pm} = \frac{1}{\pi^2} \int_0^{\infty} dk k^2 \sigma_{\pm}^S(k). \quad (9)$$

The results are shown in Fig. 6. Notice that in the parity preserving case, $\theta = 0$, the value of the condensate for each species is half the value of the ordinary condensate [9, 10]. The reason is that when fermion species are degenerate in mass, each one of them, corresponding to a fermion pairing mode $\bar{\psi}_{\downarrow}\psi_{\uparrow}$ or $\bar{\psi}_{\uparrow}\psi_{\downarrow}$ (arrows indicate spin orientation), contributes one half to the parity preserving condensate.

Finally, let us consider wavefunction renormalization effects. Regarding the wavefunction renormalization in the dynamically generated mass functions $M_{\pm}(p)$, we compare the solutions of the full systems in the previous subsection, Eq. (8), against the solution for the simplified equations resulting from the perturbation theory motivated ansatz $A_{\pm}(p) = 1$, namely

$$B_{\pm}(p) = \frac{\alpha}{\pi^2} \int d^3k \frac{B_{\pm}(k)}{k^2 + B_{\pm}^2(k)} \frac{1}{(q^2 + \theta^2)} \mp \frac{\alpha\theta}{\pi^2} \int d^3k \frac{1}{k^2 + B_{\pm}^2(k)} \frac{(k \cdot q)}{q^2(q^2 + \theta^2)}. \quad (10)$$

The behavior of the solutions in this truncation is qualitatively similar to that of the complete system (8). The critical behavior of the dynamical masses is not washed out by the effect of wavefunction renormalization, as can be seen in Fig. 7, where a comparison of μ_{\pm} and $|\mu_{+}|$ between the full result and the perturbatively motivated one is shown. The behavior is virtually the same in both truncation schemes. The critical value θ_c^{pert} is of the same order of θ_c and thus the effects of $A_{\pm}(p) \approx 1$ are not significant. This means that even with the inclusion of the CS term, the rainbow-ladder truncation is still reliable in Landau gauge.

4. Confinement

In ordinary quenched QED₃, there is confinement. Here we are interested in the extent up to which this scenario persist in the presence of a CS term. Whether a solution to the SDE supports confinement can be tested by means of the violation of the Osterwalder-Schrader axiom

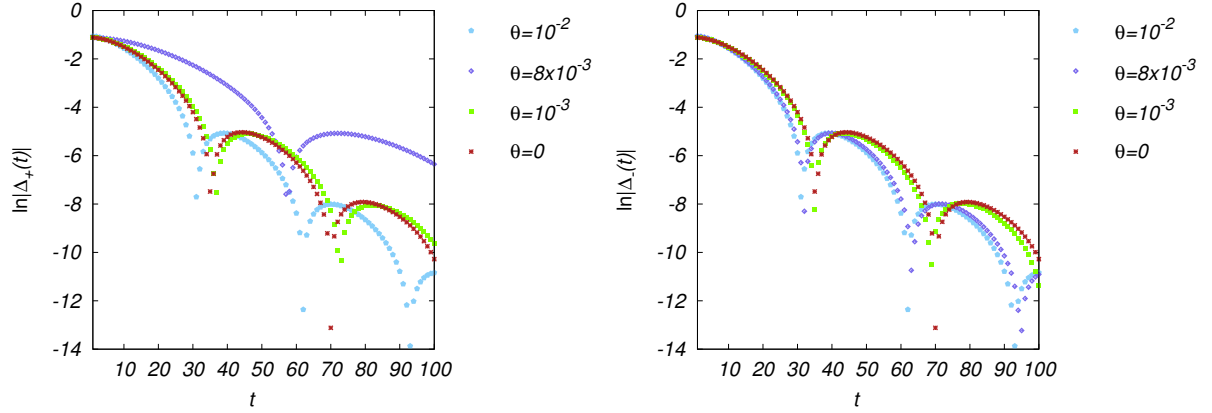


Figure 8. Confinement tests for the spatially averaged Schwinger functions.

of reflection positivity, which states that the spatially averaged Schwinger functions

$$\Delta_{\pm}(t) = \int d^2x \int \frac{d^3p}{(2\pi)^3} e^{i(tp_o + x \cdot p)} \sigma_{\pm}^S(p), \quad (11)$$

should be positive definite if they are related to a stable asymptotic state. In our case, we construct the functions $\Delta_{\pm}(t)$ inserting the solutions for the SDE in the above expression, upon which we perform a confinement test. In Fig. 8 we plot the logarithm of the absolute value of each of these functions. The oscillatory behavior inferred from the pronounced peaks in the graphs reveals that even in the presence of a CS term, quenched QED₃ exhibits confinement. This behavior corresponds to two complex conjugate mass like singularities with complex masses $m = a \pm ib$ for each species, which fit to

$$\Delta_{\pm}(t) \simeq C_{\pm} e^{-a \pm it} \cos(b_{\pm} t + \delta_{\pm}). \quad (12)$$

Thus, confinement is observed in our model.

Following Ref.[11], we perform a similar analysis on the vector parts of the propagator, σ_{\pm}^V . We define new set of spatially averaged Schwinger functions,

$$\Omega_{\pm}(t) = \int d^2x \int \frac{d^3p}{(2\pi)^3} e^{i(tp_o + x \cdot p)} \sigma_{\pm}^V(p), \quad (13)$$

and insert again the solutions found in previous sections. In Fig. 9 we draw the logarithm of the absolute values of $\Omega_{\pm}(t)$. Again, the oscillations hint confinement. Moreover, we observe that $\Omega_{\pm}(t)$ can be fitted according to

$$\Omega_{\pm}(t) \simeq C'_{\pm} e^{-a' \pm it} \cos(b'_{\pm} t + \delta'_{\pm}), \quad (14)$$

which also unveils the complex pole mass structure of the propagator.

5. Conclusions

We have studied the dynamical generation of masses and confinement in Maxwell-Chern-Simons QED₃. There exists two types of fermions within the four-component spinor formalism. These species are non-degenerated in mass. The origin of these physical masses is two-fold: On the

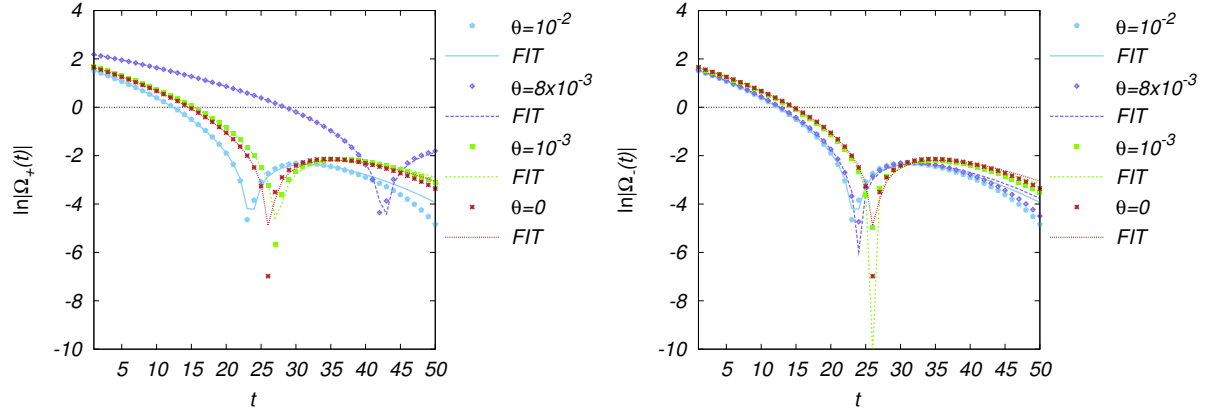


Figure 9. Spatially averaged Schwinger functions involving the vector parts of the fermion propagator.

one hand there is a parity-preserving contribution m_e coming from dynamical chiral symmetry breaking, on the other hand, there is the CS-induced Haldane mass term m_o . We have explored the consequences of confinement in our model.

For $\theta > \theta_c$ the masses for each species are equal in magnitude, $\mu_+ = -\mu_-$, and we do not generate the ordinary mass $\mu_e = (\mu_+ + \mu_-)/2$ that preserves parity. This is the reason why there is restoration of chiral symmetry and we only generated masses induced by the CS term. The phase transition for the mass μ_+ is of first order. Regarding confinement, according to tests performed with σ^V and σ^S , we observe that quenched QED₃ with a CS term also shows this feature, regardless the value of the CS coefficient. This is in contrast to the case in which vacuum polarization effects are considered in the leading order of the $1/N$ approximation [11], where there is deconfinement for arbitrary finite values of θ .

Acknowledgments

We acknowledge support from SNI, CIC, and CONACyT grants through projects 4.22, 82230, and 50744-F, respectively.

References

- [1] K.-I. Kondo and P. Maris 1995 *Phys. Rev. Lett.* **74** 18
- [2] K.-I. Kondo and P. Maris 1995 *Phys. Rev. D* **52** 1212
- [3] T. Appelquist, M. Bowick, D. Karabali and L.C.R. Wijewardhana 1986 *Phys. Rev. D* **33** 3704
- [4] R.D. Pisarski 1984 *Phys. Rev. D* **29** 2423
- [5] G.W. Semenoff and L.C.R. Wijewardhana 1988 *Phys. Rev. Lett.* **62** 2633
- [6] K. Shimizu 1985 *Prog. Theor. Phys.* **74** 610
- [7] Ma. de J. Anguiano and A. Bashir 2005 *Few Body Syst.* **37** 71
- [8] F. D. M. Haldane 1988 *Phys. Rev. Lett.* **61** 2015
- [9] C.D. Roberts and A. G. Williams 1994 *Prog. Part. Nucl. Phys.* **33** 477
- [10] A. Bashir and A. Raya 2007 *Few Body Syst.* **41** 185
- [11] C.P. Hofmann, A. Raya and S. Sánchez Madrigal 2010 *Phys. Rev. D* **82** 096011